

2015•2016
FACULTEIT GENEESKUNDE EN LEVENSWETENSCHAPPEN
master in de biomedische wetenschappen

Masterproef

Establishment and characterization of high-grade serous ovarian cancer models to study the role of metabolic adaptations in platinum resistance

Promotor :
Prof. dr. Ivo LAMBRICHTS

Promotor :
Prof. dr. FRÉDÉRIC AMANT
dr. DANIELA ANNIBALI

Jelle Stans

Scriptie ingediend tot het behalen van de graad van master in de biomedische wetenschappen

De transnationale Universiteit Limburg is een uniek samenwerkingsverband van twee universiteiten in twee landen: de Universiteit Hasselt en Maastricht University.



Universiteit Hasselt | Campus Hasselt | Martelarenlaan 42 | BE-3500 Hasselt
Universiteit Hasselt | Campus Diepenbeek | Agoralaan Gebouw D | BE-3590 Diepenbeek



Maastricht University

2015•2016
FACULTEIT GENEESKUNDE EN
LEVENSWETENSCHAPPEN
master in de biomedische wetenschappen

Masterproef

Establishment and characterization of high-grade serous ovarian cancer models to study the role of metabolic adaptations in platinum resistance

Promotor :
Prof. dr. Ivo LAMBRICHTS

Promotor :
Prof. dr. FRÉDÉRIC AMANT
dr. DANIELA ANNIBALI

Jelle Stans

Scriptie ingediend tot het behalen van de graad van master in de biomedische wetenschappen

Table of contents

List of abbreviations	iii
Acknowledgements	v
Abstract	vii
Samenvatting.....	ix
1. Introduction.....	1
1.1. Ovarian cancer: general overview and epidemiology	1
1.2. High-grade serous ovarian carcinoma.....	1
1.2.1. Molecular characterization of high-grade serous ovarian carcinoma	1
1.3. Treatment of high-grade serous ovarian carcinoma.....	1
1.3.1. Surgery.....	1
1.3.2. Platinum-based chemotherapy	2
1.3.3. Taxanes.....	3
1.4. Resistance against platinum-based chemotherapy	3
1.5. Molecular basis of platinum resistance.....	4
1.6. Models to investigate therapy resistance	5
1.6.1. In vitro models.....	5
1.6.2. In vivo models.....	5
1.7. Objectives	6
2. Materials & methods.....	9
2.1. Cell lines and culture	9
2.2. Mice.....	9
2.3. Tumor implantation	9
2.4. Animal treatment	9
2.5. Biopsy procedure.....	10
2.6. Sacrifice and sample collection	10
2.7. Sample processing.....	10
2.8. Cell line carboplatin treatment	10
2.9. Primary cell isolation and carboplatin treatment	10
2.10. Histology.....	11
2.11. Immunocytochemistry	11
2.11.1. Human vimentin and pan-cytokeratin	11
2.12. Statistics.....	12
3. Results	13
3.1. Carboplatin response of 2 HGSC cell lines.....	13

3.1.1.	Dose escalation experiment	13
3.1.2.	Cell growth analysis	14
3.1.3.	Determination of 50% growth inhibition concentration (GI50)	15
3.1.4.	Cell growth under selected experimental conditions	16
3.2.	Carboplatin response of 3 PDTX models	17
3.2.1.	Platinum-resistant model (OVC005).....	19
3.2.2.	Platinum-sensitive model (OVC020)	21
3.2.3.	Relapse model (OVC034).....	22
3.3.	Primary PDC culture establishment and carboplatin response	23
3.3.1.	Optimization of culture protocol.....	23
3.3.2.	Determination of growth rate	24
3.3.3.	Determination of 50% growth inhibition concentration (GI50)	25
4.	Discussion	27
4.1.	Carboplatin response of HGSC cell lines.....	27
4.2.	Carboplatin response of PDTX models	28
4.3.	Primary PDC culture establishment and carboplatin response	29
5.	Conclusion	31
	References.....	33

List of abbreviations

ATP7B:	ATPase, Cu ²⁺ transporting, β polypeptide
ATR:	ATM- and RAD3-related protein
BRCA1:	Breast cancer 1
BRCA2:	Breast cancer 2
CCC:	Clear cell carcinoma
CDDP:	<i>Cis</i> -diamminedichloridoplatinum(II), cisplatin
CDK12:	Cyclin-dependent kinase 12
CHECK1:	Checkpoint kinase 1
CGARN:	Cancer genome atlas research network
CSMD3:	CUB and Sushi multiple domains protein 3
CTR1:	Copper transporter 1
DAPI:	4',6-Diamidino-2-Phenylindole, Dihydrochloride
EGF:	Epidermal growth factor
EOC:	Endometroid ovarian carcinoma
FAT3:	FAT atypical cadherin 3
FBS:	Fetal bovine serum
GABRA6:	Gamma-aminobutyric acid A receptor, Alpha 6
GC-MS:	Gas chromatography – mass spectrometry
GEMM:	Genetically engineered mouse model
GSTP1:	Glutathione S-transferase P1
H&E:	Haematoxylin & eosin
HGSC:	High-grade serous ovarian carcinoma
HR:	Homologous recombination
LGSC:	Low-grade serous ovarian carcinoma
MMR:	Mismatch repair
MOMP:	Mitochondrial outer membrane permeabilization
MRD:	Minimal residual disease
NER:	Nucleotide excision repair
NF1:	Neurofibromin 1
NGS:	Next Generation Sequencing
OCMI:	Ovarian Carcinoma Modified Ince medium
OVC:	Ovarian cancer
PBS:	Phosphate buffered saline
PDC:	Patient-derived tumor xenograft-derived cell culture
PDH:	Pyruvate dehydrogenase
PDTX:	Patient-derived tumor xenograft
PFI:	Platinum-free interval
RB1:	Retinoblastoma 1
RPMI:	Roswell Park Memorial Institute Medium
SPF:	Specific pathogen free
VEGF:	Vascular endothelial growth factor

Acknowledgements

A master's thesis is the final chapter of a whole trajectory at the university and guides the way of a scientist's future career. That's why I would like to thank my promotor Prof. dr. Frédéric Amant for allowing me to join the laboratory of gynaecological oncology for 30 weeks and introducing me to the world of cancer research.

I owe a lot of gratitude to my daily supervisor dr. Daniela Annibali for the experimental guidance, willingness to answer all my questions during the internship and revision of my drafts. Her input was indispensable for the realization of this thesis.

I would also like to thank my institutional supervisor Prof. dr. Ivo Lambrichts and second examiner Prof. dr. Virginie Bito for their valuable input and evaluating this thesis.

Tom, thanks for the excellent team work and being flexible whenever I had other obligations. This internship would have been a lot harder and less rewarding if you hadn't been there. Also thanks to Stijn, Tina, Tine and all the other people in the gynaecological oncology lab that taught me different techniques and took care of the good working atmosphere, and to Ellen and Debby of the TRACE platform.

My parents, brothers and sister have always supported me throughout the years, for which I am very grateful.

Last, but absolutely not least, I would like to thank my friends. Katrien, Anoeshka, Melina, Jolien, Frauke, Lien, Saskia, Kathleen, Iris and everybody else: thanks for making my time in Diepenbeek and Leuven an unforgettable experience!

Abstract

Platinum-based chemotherapy is the standard of care for high-grade serous ovarian carcinoma (HGSC). High initial response rates are often followed by relapse and gradual development of resistance. The molecular mechanisms responsible for the development of platinum resistance are not completely understood yet and Next Generation Sequencing techniques failed to identify contributing point mutations. One promising hypothesis is that metabolic alterations connected to pathways controlling cell death are involved. To identify metabolic adaptations linked to platinum resistance, relevant models of HGSC are required. In the present study we established and characterized models of HGSC to develop tools for future use in the identification of metabolic alterations responsible for platinum resistance in HGSC.

We characterized the platinum response of A2780 and A2780 cis, 2 HGSC cell lines, to validate them as an in vitro model for future metabolomics experiments. Additionally, we treated patient-derived tumor xenografts (PDX) models of 3 different tumours with carboplatin to confirm their validity as an in vivo model. A biopsy procedure was tested as a sample collection method. From 1 PDX model, we established and characterized primary PDX-derived cell (PDC) cell cultures.

The characterization of the cell lines' response to carboplatin revealed the optimal experimental conditions for future metabolomics experiments. The PDX models' response to treatment mirrored the one observed for the respective patients. The biopsy procedure did not alter tumor growth. Primary PDC cultures were established and shown to mirror the PDX model's response to carboplatin.

The characterization of the HGSC cell lines provides an in vitro model that can be used to perform metabolomics experiments, including labeled tracer analysis. The results of these experiments will subsequently be validated in the patient-derived in vitro and in vivo models established and characterized in the present study.

Samenvatting

Platinum gebaseerde chemotherapie is de standaardtherapie voor hooggradig, sereus ovariumcarcinoom (HGSC). Hoge initiële responsratio's worden vaak gevolgd door herval en graduele ontwikkeling van resistentie. De moleculaire mechanismen die verantwoordelijk zijn voor het ontstaan van platinum resistentie zijn nog niet volledig ontrafeld en Next Generation Sequencing technieken konden geen bijdragende puntmutaties identificeren. Een veelbelovende hypothese is dat metabole veranderingen die gelinkt zijn aan celdood-controlerende pathways een rol spelen. Om metabole veranderingen die gelinkt zijn aan platinum resistentie te kunnen identificeren, zijn relevante modellen van HGSC nodig. In deze studie ontwikkelden en karakteriseerden we HGSC modellen voor toekomstig gebruik in het identificeren van metabole veranderingen die verantwoordelijk zijn voor platinum resistentie in HGSC.

We karakteriseerden de platinum respons van A2780 en A2780 cis, 2 HGSC cellijnen, om ze te valideren als een in vitro model voor toekomstige metabolomics experimenten. Daarnaast behandelden we patient-derived tumor xenograft (PDX) modellen van 3 verschillende tumoren met carboplatinum om hun bruikbaarheid als een in vivo model na te gaan. Een biopsieprocedure werd getest als staalcollectiemethode. Van 1 van de PDX modellen werden primaire PDX-derived celculturen (PDC) opgezet en gekarakteriseerd.

De karakterisatie van de HGSC cellijnen toonde de optimale experimentele condities voor toekomstige metabolomics experimenten. De behandelingsrespons van de PDX modellen was gelijkaardig aan die van de overeenkomstige patiënten. De biopsieprocedure had geen invloed op tumorgroei. Primaire PDC culturen werden opgezet. Hun carboplatinumrespons was gelijkaardig aan die van de PDX modellen waarvan ze afkomstig zijn.

De karakterisatie van de HGSC cellijnen zorgt voor een in vitro model dat gebruikt kan worden voor metabolomics experimenten, waaronder labeled tracer analyse. The resultaten van deze experimenten zullen daarna worden gevalideerd in de patient-derived in vitro en in vivo modellen die werden opgezet en gekarakteriseerd in de huidige studie.

1. Introduction

1.1. Ovarian cancer: general overview and epidemiology

Ovarian cancer annually affects over 200,000 newly-diagnosed women worldwide. In 2012, over 150,000 individuals were estimated to have died from this malignancy (1, 2). This makes ovarian cancer the fourth most lethal cancer in females and the leading cause of gynaecological cancer-associated death in the developed world (3, 4).

Historically, ovarian cancer was thought to be a single disease. However, the term 'ovarian cancer' is today used to refer to a heterogeneous set of diseases (5) that can be subdivided in epithelial (90% of all cases (6)) and non-epithelial variants, both with their own subtypes. For the epithelial cancers, these subtypes are: high-grade serous carcinoma (HGSC), low-grade serous carcinoma (LGSC), endometrioid ovarian carcinoma (EOC) and clear cell carcinoma (CCC). Non-epithelial ovarian cancer consists of sex-cord stromal, germ cell and steroid cell tumors (7-10).

1.2. High-grade serous ovarian carcinoma

The most common subtype, HGSC, comprises over 70% of all newly diagnosed cases of ovarian cancer (10) and accounts for most of its mortality (11, 12). High-grade carcinomas have a worse prognosis than low-grade tumors (13).

An important cause of HGSC's lethality is the late stage at which the disease is usually diagnosed. When patients present to the clinician, their cancer is often already spread in the abdomen and to distant organs (3, 4). This translates into a 5-year survival of only 40% (7). In contrast to other solid tumor types like breast cancer, the prognosis for ovarian cancer patients has not improved in the last 15-20 years (14-16).

1.2.1. Molecular characterization of high-grade serous ovarian carcinoma

HGSCs are characterized by p53 mutations in almost all cases (12, 17). BRCA1 and BRCA2 mutations are more common in HGSC than in other subtypes (12). Other significantly mutated genes are CDK12, CSMD3, FAT3, GABRA6, NF1 and RB1 (12). The Cancer Genome Atlas Research Network (CGARN) has divided HGSC further into differentiated, immunoreactive, mesenchymal and proliferative subtypes (12).

1.3. Treatment of high-grade serous ovarian carcinoma

Standard of care treatment for advanced high-grade serous ovarian carcinomas is surgery and platinum-based chemotherapy, alone or in combination with taxane(s). Most often, a combination of carboplatin and paclitaxel is used (4, 18).

Despite the high response rates observed after first-line treatment (19), about 30% of all patients with HGSC relapse within 6 months (5) and 70% of all patients with ovarian cancer within 3 years (6). The different treatment strategies will be discussed separately in the following paragraphs.

1.3.1. Surgery

As first-line treatment, surgery is performed for a variety of reasons: **(1)** First of all, surgery allows histological diagnosis (4, 20). **(2)** Secondly, surgery allows staging of the tumor (4, 20). **(3)** Finally,

resection of tumor tissue ('debulking surgery') has been linked to improved survival in newly diagnosed, chemo-naive patients (4, 18, 21).

1.3.2. Platinum-based chemotherapy

Platinum-based chemotherapy has been used for ovarian cancer over the last 4 decades and is still standard of care treatment today (4). Originally, cisplatin (*cis*-diamminedichloridoplatinum(II), CDDP) was used (22). In 1992 carboplatin (*cis*-diammine(1,1-cyclobutanedicarboxylato)platinum(II)), a less toxic analogue of cisplatin, was introduced (23, 24).

In relapsed patients, additional platinum-based chemotherapeutic treatment can be decided, based on the tumor's sensitivity, since time between the last dose of received chemotherapy and clinically evident relapse (platinum-free interval, PFI) has been correlated with response to additional chemotherapeutic treatment(6, 10). It may not be worth exposing specific patients to toxic chemotherapy, when this is not likely to inhibit progression of their disease (25).

Cisplatin and carboplatin have identical methods of actions (Figure 1) (26). These chemotherapeutics exert their effects (cell cycle arrest and/or cell death) by a number of different mechanisms, which are not completely understood yet (26, 27). **(1)** First of all, they bind to DNA, mainly on N7 sites on DNA purines, forming intrastrand DNA-DNA adducts and inducing apoptosis (26). This mechanism is the most important mechanism of the platinum-based compounds' cytotoxicity. **(2)** Secondly, they promote oxidative stress by lowering the cytosolic concentration of reducing equivalents, which favors oxidative stress and has a cytotoxic effect (26).

The toxicity of platinum-based chemotherapeutics is mediated by the activation of ATM- and RAD3-related protein (ATR), leading to the activation of checkpoint kinase 1 (CHEK1). Eventually, this leads to the phosphorylation of p53, inducing cell cycle arrest, or cell death by mitochondrial outer membrane permeabilization (MOMP) (26).

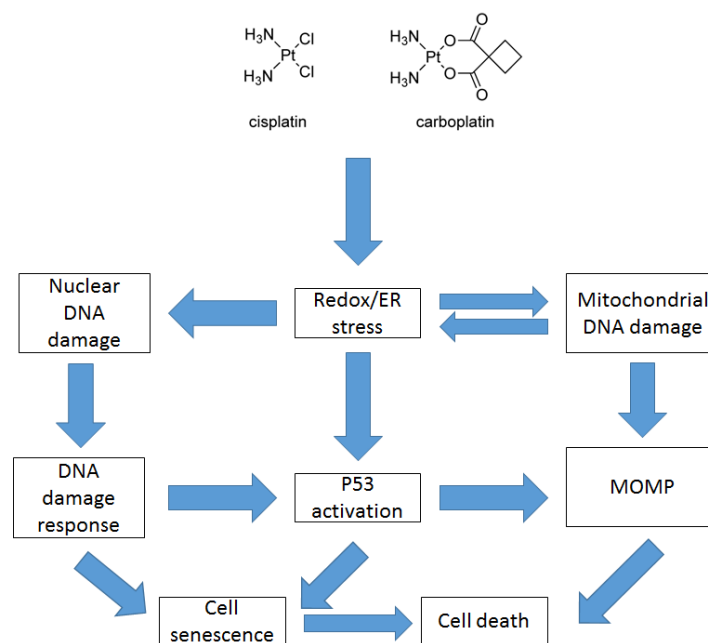


Figure 1: Methods of action of cisplatin and carboplatin. Adapted from Galluzzi et al. (2014) (26). ER: endoplasmic reticulum, MOMP: mitochondrial outer membrane permeabilization

1.3.3. Taxanes

In 1996, it was discovered that adding paclitaxel to the platinum-containing regimen improves survival in patients with advanced disease (28). Thus, taxanes are presently combined with platinum-containing compounds to manage chemo-naïve ovarian cancers (4). These compounds are cytoskeletal drugs that target tubulin to prevent microtubule breakdown. In this way they are able to block mitosis and eventually trigger apoptosis (29).

1.4. Resistance against platinum-based chemotherapy

Based on the time between the last treatment and progression of disease, the so-called platinum-free interval (PFI), tumors can be divided into different classes (10). When the PFI is longer than 6 months, the disease is considered platinum sensitive and it is usually re-treated with platinum. When the disease progresses within 6 months after treatment completion, it is 'platinum resistant'. When the cancer progresses during treatment, it is deemed 'platinum refractory' (10). In both case, a new platinum line is considered less likely to be effective and not used, leaving the patients with limited treatment options.

The mechanisms by which platinum-resistance develops, or is initially present, are not completely understood. However, there are at least 4 different proposed classes of mechanisms used by cancer cells to avoid platinum-mediated toxic effects (Figure 2)(26).

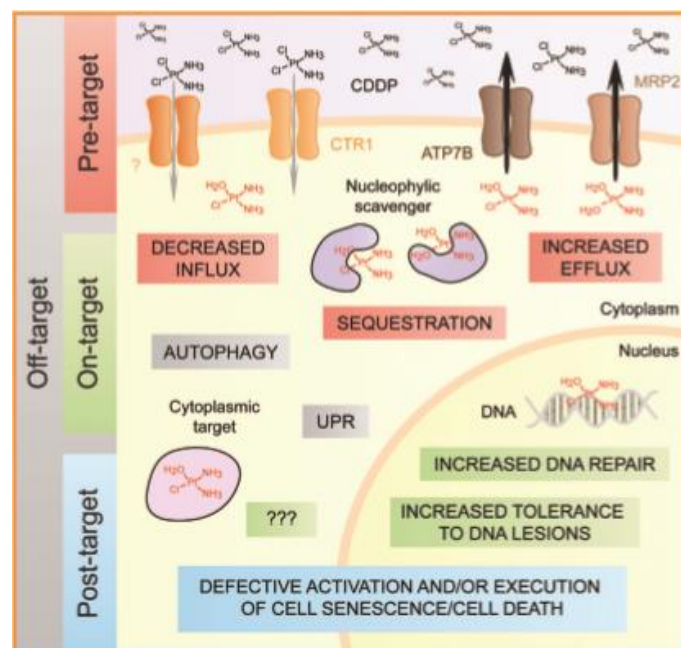


Figure 2: Resistance mechanisms to cisplatin and carboplatin. Galluzzi et al. (2014)(26)

(1) Pre-target mechanisms include the reduction of the active (aquated) compound in the cytoplasm (26). This can be caused by a downregulation or inactivation of transporters that move the compound out of the cytoplasm, like copper transporter 1 (CTR1) (30). Another way is the upregulation of transporters like the ATPase, Cu^{2+} transporting, β polypeptide, (ATP7B) (30). Higher levels of enzymes that chelate platinum can also contribute to platinum resistance (31). **(2)** On-target

mechanisms are alterations at the DNA-level, which is the primary target of platinum-based chemotherapeutics (26). The 3 main DNA repair pathways have been proposed to be involved: nucleotide excision repair (NER), mismatch repair (MMR) and homologous recombination (HR)(26, 32, 33). **(3)** Post-target mechanisms consist of alterations that impair the detection of platinum-induced damage or the execution of cell death (26). Examples include genetic and epigenetic alterations in the P53 pathway (26). **(4)** Off-target mechanisms consist of activation of alternative survival signals which are not a direct consequence of the platinum-based chemotherapeutics, for example autophagy (34) and the heat shock response (35).

1.5. Molecular basis of platinum resistance

Platinum resistance has been studied for over 4 decades, without much success in improving the management of resistant diseases (26). Recently, the introduction of high-throughput technologies like Next Generation Sequencing (NGS) provided important insights (12). However, it is still extremely challenging to accurately predict platinum responsiveness (10).

In 2014, a link was suggested between metabolic rearrangements and pathways involved in cell death programming (14). This link consists of several components (figure 3).

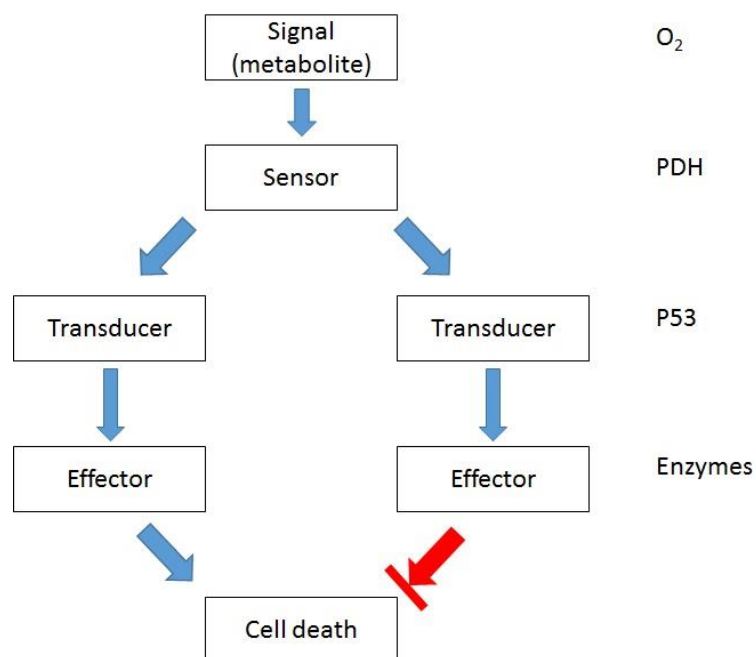


Figure 3: Metabolic control of cell death. Adapted from Green et al. (2014) (14) PDH: pyruvate dehydrogenase

Shifts in metabolite concentrations act as signals (e.g. O₂, succinate) **(1)** that are detected by specific sensors (e.g. PDHs) **(2)**. These sensors pass these signals through transducers (e.g. p53) **(3)** which will cause effectors (e.g. specific enzymes) **(4)**, as part of the cell death machinery, to stimulate cell survival or apoptosis (14). In this view, an interesting hypothesis is that specific cellular metabolic alterations might be linked to platinum resistance in HGSCs. In vitro experiments have already shown that platinum administration to cell lines can alter gene expression of essential metabolic pathway components. Metabolic alterations are linked to chemotherapeutic resistance in breast cancer (36). Poisson et al. (37) have identified metabolic

alterations in platinum-resistant cell lines that may play a role in the development of their resistance. These alterations were found in major pathways that appeared to be interconnected: the methionine-cysteine metabolism (part of the one-carbon metabolism) and associated glutathione synthesis pathways contained the most significantly altered metabolites. Other researchers (38) found that expression of an important platinum-drug metabolising enzyme, glutathione S-transferase P1 (GSTP1), is linked to drug sensitivity in ovarian cancer cell lines.

There is less data from in vivo experiments on the role of metabolism in development of drug resistance in cancer. Recently, Pommier et al (39) suggested a correlation between a specific metabolic gene expression signature and resistance to VEGF inhibition in patients with metastatic colorectal cancer.

To investigate potential molecular causes of therapeutic failure, researchers can use a variety of models, which will be discussed in the following paragraph.

1.6. Models to investigate therapy resistance

Cancer research, including research into chemotherapeutic resistance, is carried out in different models. (40). In vitro models are used to obtain new information about the molecular mechanisms involved in cancer and identify new therapeutics (41). The results obtained with these models need to be subsequently validated in pre-clinical in vivo models.

1.6.1. In vitro models

(1) Immortalized cell lines are used for a variety of experiments, including pre-clinical drug screenings (42). A fundamental drawback of these cell lines is their lack of resemblance to the human tumor cells populating the cancer mass in vivo (42). Growing in culture induces genetic and metabolic alterations, which enable them to grow in this condition. When these cells are injected into mice, the resulting tumor xenograft tissue does not always resemble a human tumor (40). **(2)** Secondly, cells derived from patients can be also used (43). In this approach, cells are isolated from human tissue material and grown in 3D in vitro conditions. They are cultured with an ECM substitute like Matrigel and a variety of growth factors (43). These so-called organoids are a near-physiological model system that approaches in vivo conditions much better than regular cell lines (43).

1.6.2. In vivo models

(1) Genetically engineered mouse models (GEMM) are an important in vivo model in cancer research. They are generated by genetic techniques by introducing oncogenes and/or knocking out tumor suppressor genes. These models can be used to investigate tumorigenesis and the interaction between cancer cells and the tumor microenvironment (44). **(2)** Alternatively, fragments of a patient's tumor can be implanted into immune-deficient mice to generate patient-derived tumor xenograft (PDX) models.

These PDX models are established by transplanting tumor freshly-isolated surgical specimens into immune-compromised mice. Tumor cells in the transplanted tissue proliferate and propagate the original tumor. This tumor can subsequently be explanted and re-transplanted into a new generation of mice. It has been shown that, after multiple transplants, the PDX tumor still resembles the donor tumor at the histologic, genetic and transcriptomic level. These models can also be pharmacologically validated by treating them with a specific treatment (e.g. the standard of care used in the clinic) and looking whether the model recapitulates the treatment response observed in the original patient

(40). For many different tumor types, PDX models have a high predictive value in terms of response to therapy (40, 45).

PDX models also have several limitations (40). **(1)** First, they lack a functional immune system. Nude mice, a type of immune-compromised mice often used to establish PDX models, do not possess T-cells. This means that an important component of the tumor microenvironment cannot be studied in these models (46). **(2)** Secondly, some tumors have a relatively low take rate. It has been suggested that more aggressive tumors have a higher take rate (46). **(3)** Thirdly, human stroma is largely replaced by murine stroma after several passages (40). This poses problems for research into tumor microenvironment components, including blood vessels and immune cells. **(4)** Finally, technical challenges such as the selection of the optimal transplantation site, should be considered. Different possibilities are an implantation in the interscapular fat pad below the skin (subcutaneous implantation) or in the organ where the tumor derived from (orthotopic implantation). It has been shown that, for different tumors, these different sites can yield different success rates (40, 46).

PDX models have been established for a number of cancer types, including: colorectal, pancreatic, lung and ovarian cancer (40).

1.7. Objectives

High-throughput metabolomics and transcriptomics techniques allow for the identification of metabolites concentration in tissue samples. The power of these technologies can be fully exploited when there are combined with relevant pre-clinical models. The goal of the current project was to establish and characterize HGSC models that can be used to investigate metabolic alterations linked to platinum resistance using metabolomics (gas chromatography – mass spectrometry, GC-MS) and transcriptomics (RNAseq) techniques.

Objectives:

1. Characterize the platinum response of 2 HGSC cell lines and determine optimal conditions for future metabolomics experiments.
2. Validate the platinum response of 3 different PDX models.
3. Establish and characterize primary PDX-derived cell (PDC) cultures from the PDX-models.

Characterize the platinum response of 2 HGSC cell lines and determine optimal conditions for future metabolomics experiments

The response to carboplatin of 2 HGSC cell lines, A2780 (platinum-sensitive) and A2780 cis (platinum-resistant) was characterized. Subsequently, the optimal experimental conditions for a labeled tracer experiment using these cell lines were determined.

Validate the platinum response of 3 PDX models and test a biopsy procedure

3 previously established PDX models were treated with carboplatin to assess whether their response mirrored that of the original patient. These models were OVC005, OVC020 and OVC034, respectively established from a platinum-resistant, sensitive and lymph node relapse tumor. OVC020 and OVC034 originated from the same patient. Additionally, a biopsy procedure was tested to collect tumor samples before, during and after treatment for future metabolomic analysis.

Establish and characterize primary PDC cultures from PDTX-models

From 1 PDTX model, primary cell cultures were established and their response to carboplatin was characterized.

In conclusion, the characterization of the HGSC cell lines provides an in vitro model that can easily be used to perform metabolomics experiments. The results of these experiments can subsequently be validated in the patient-derived in vitro and in vivo models established and characterized in the present study.

2. Materials & methods

2.1. Cell lines and culture

A2780 and A2780 cis (Sigma – Aldrich) cell lines. Were grown in Roswell Park Memorial Institute (RPMI) medium supplemented with 10% fetal bovine serum (FBS), 100 U/ml penicillin and 100 µg/ml streptomycin, 2 µM L-glutamine. (4°C). All cell lines were kept in a CO₂ incubator (Sanyo) at 37°C and 5% CO₂. When cells became too confluent, a subculture was performed. This was done by aspirating the medium and washing with PBS. The cells were then detached by adding 0.25% trypsin (0.05% for primary cells) and incubating for 5 minutes at 37°C and 5% CO₂. The trypsin was inactivated by adding RPMI medium supplemented with FBS. The cell solution was then transferred to a falcon tube and centrifuged (Eppendorf centrifuge 5810 R) for 5 minutes at 1200 rpm. The supernatant was removed and the cells were resuspended in RPMI medium supplemented as before. This solution was then divided over different flasks and put into culture. Twice a week, the medium in each flask was replaced.

Fibroblasts were removed from primary cultures by differential trypsinization when threatening epithelial cell growth. This was done using the subculture protocol using 0.05% trypsin. Cells were visualized using a Leica DFC 295 microscope.

2.2. Mice

Female, nude NMRI mice (BomTac:NMRI-*Foxn1^{nu}*) (Taconic) were used. Animals were kept in individually ventilated cages in a semi-specific pathogen free facility, with ad libitum access to food and water.

Procedures involving animals were performed in accordance with the guidelines of the Catholic University of Leuven (KU Leuven) Animal Care and Use Ethical Committee ((P147/2012 and P038/2015).

2.3. Tumor implantation

The tumor implantation was performed in a laminar flow located in a semi-SPF facility. Animals were sedated with an intraperitoneal injection of a 70 mg/kg ketamine- medetomidine solution. The animal was transferred to another laminar flow and placed on a heating pad (37°C). Afterwards, the surgical area was disinfected with 7.5% Braunol and 70% ethanol. An incision was made in the skin above the interscapular fat pad. The interscapular fat pad was exposed and punctured. A tumor fragment (3x3 – 5x5 mm) was placed into the hole. The fat pad was placed back in its original position and the wound was closed with a Michel suture clip. 100 µl of a 0.3 mg/ml buprenorphine solution was subcutaneously injected into each flank, to provide analgesic support. A subcutaneous 10 µl/10 g injection of a 5 mg/ml Atipamezole solution, to reverse the anesthesia, was given and animals were kept on the heating pad until fully regaining consciousness.

2.4. Animal treatment

Mice were randomly assigned to receive treatment or placebo when their tumor volume reached about 425 mm³. After inclusion, the animals were treated once a week, for 3 weeks with a 26,936 µM carboplatin solution (treatment group) or a 0.9% saline solution (placebo group). Tumor dimensions were measured in vivo twice a week using a caliper. The tumor volume was calculated according to the following formula: length x (width) ² x π / 6.

2.5. Biopsy procedure

Animals were sedated by an intra-peritoneal injection of a 75 mg/kg ketamine, 100 mg/kg medetomidine solution and kept on a heating pad (38°C). 100 µl of a 0.3 mg/ml buprenorphine solution was subcutaneously injected into the flank, to provide analgesic support. The surgical area was disinfected with Braunol and 70% ethanol. Subsequently, an incision was made in the skin above the tumor. Tumor membrane was accessed through this incision and cut. A 2.5 mm punch biopsy needle was inserted into the tumor and slowly rotated. The resulting biopsy was squeezed with a liquid nitrogen pre-cooled tissue squeezer and snap-frozen. The wound was closed with clips and the same 100 µl buprenorphine solution was injected into the opposite flank. The animals were given a subcutaneous 10 µl/10 g injection of a 5 mg/ml Atipamezole solution, to reverse the anesthesia, and were placed back in their cage when they fully regained consciousness.

2.6. Sacrifice and sample collection

The animals were sedated by an intra-peritoneal injection of a 125 mg/kg ketamine, 166 mg/kg medetomidine solution. After in vivo measurement, the tumor was resected, measured ex vivo and weighed. The tumor was fragmented. Subsequently, blood was collected with a cardiac puncture. Afterwards, the animals were sacrificed by cervical dislocation. During dissection lung lobes, apparent lymph nodes and macroscopic metastasis were collected.

2.7. Sample processing

Tumor fragments were either squeezed by using a liquid nitrogen pre-cooled tissue squeezer and snap-frozen in liquid nitrogen (for metabolites analysis), or placed RNA-later (for RNA analysis), distributed over cryotubes and snap-frozen (for protein analysis) or placed in a 4% M/V formaldehyde solution (for histological analysis).

Collected blood was immediately mixed with heparin and afterwards centrifuged for 8 minutes at 5,000 rpm (Eppendorf centrifuge 5418). The supernatant (serum) was transferred to a new cryotube. A single lung lobe was snap-frozen. The remaining lung lobes and the collected lymph nodes were placed in the formaldehyde solution.

All frozen samples, the RNA-later container and serum were stored at -80°C. After 24 hours, the samples placed in formol were washed with PBS and stored in 70% ethanol at room temperature.

2.8. Cell line carboplatin treatment

For A2780 and A2780 cis cell lines, 35,000 cells were seeded in different wells and exposed to RPMI medium + 10% with or without 6µM of carboplatin, 1 day after attachment. Live and dead cells were counted daily by using an hemocytometer after trypan blue staining to assess total number of cells and dead cell fraction at each time point.

To determine the 50% growth inhibition concentration, 25,000 cells were seeded in different wells for each cell line. After attachment, the cells were exposed to differential carboplatin concentrations. Live and dead cells were counted at 3 days after carboplatin treatment.

2.9. Primary cell isolation and carboplatin treatment

Primary cells were isolated from tumors grown in PDTX models using an in-house optimized protocol. Specifically, the tumor was washed in 1X PBS plus Pen/Strep and minced with a scalpel. 20 ml of a dissociation mix consisting of: 4% 10X human Collagenase/Hyaluronidase, 10% BSA fraction V, 26%

33.5:1 DMEMF12/HEPES solution, 5 µg/µl insulin and 40% 1000X gentamycin was added to the minced tumor. Subsequently, the sample was placed at 37°C in rotation for 60 minutes and then centrifuged at 425g for 5 minutes at 4°C. DMEMF12 was added and the sample was centrifuged as before. The supernatant was discarded and the pellet resuspended in pre-warmed trypsin/EDTA. Cold HF medium consisting of Hank's balanced salt solution (HBBS) supplemented with 2% FBS and 2% HEPES was added and the sample was centrifuged as described before. The supernatant was removed and a solution of pre-warmed 5 mg/mL Dispase and 1 mg/mL DNase I was added. Cold HF medium was added and the sample was centrifuged as before. The supernatant was removed and the pellet resuspended in a 1:4 mix of cold HF-medium:ammonium chloride. The sample was centrifuged as before and the supernatant removed. For adherent cultures, the pellet was washed in Ovarian Carcinoma Modified Ince (OCMI) medium consisting of a 1:1 mixture of HAM'sF12:M199 media, supplemented with 10 ng/ml EGF, 20 µg/mL insulin, 500 ng/ml hydrocortisone, 25 ng/ml cholera toxin and 2% FBS and centrifuged as before. After discarding the pellet, the pellet was resuspended in OCMI-medium and the solution was plated. For 3D/spheroid cultures, the pellet was washed in serum-free OCMI medium and centrifuged as before. The pellet was resuspended in serum-free OCMI medium and the solution was plated and placed into culture.

Primary cells were characterized using a modified version of the protocol used to characterize the A2780 and A2780 cis cell lines: 45,000 cells were seeded in each well to determine growth total cell number, doubling times and dead cell fraction. Cells were counted each other day, for 8 days. For the GI50 determination; 50,000 cells were initially seeded in each well.

2.10. Histology

Samples stored in 70% ethanol were subsequently embedded in paraffin. Paraffin blocks were stored in -20°C until they were cut into 4µM slides using a Microm HM340E microtome (Thermo scientific). Slides were dried at 37°C.

For H&E staining, slides were placed in a stove for 60 minutes at 55°C. Afterwards, they were placed in different liquid baths in the following order: Toluol (2x 5 minutes), Ethanol (2x 5 minutes), Hematoxylin solution (4 minutes) 1% HCl in 100% ethanol (briefly), LiCO₃ (briefly), Eosine (3 minutes). Subsequently, the slides were dehydrated in 100% alcohol and Xylene. Finally, the slides were mounted and dried overnight. Pictures were taken using an Axioskop microscope (Carl Zeiss AG, Germany).

2.11. Immunocytochemistry

2.11.1. Human vimentin and pan-cytokeratin

Cells were seeded on a sterile glass coverslip and washed with DPBS when 30% confluency was reached. Subsequently, the cell were fixed with 4% M/V formaldehyde for 10 minutes at room temperature. The cells were incubated for 1 hour at room temperature with 1X DPBS + 1% BSA + 0.3% Triton + 5% Donkey Serum (Sigma D9663-10ML). Afterwards, they were incubated with an anti-vimentin primary antibody (CST D21H3 Rabbit mAb) (dilution: 1:100) in 1X DPBS + 1% BSA + 0.3% Triton, overnight at 4°C. Coverslips were rinsed 3 times with 1X DPBS for 5 minutes each. They were subsequently incubated with Donkey anti-rabbit Alexa Fluor 594 (red) (Molecular Probes

A21207) (Dilution 1:600) in 1X DPBS + 1% BSA + 0.3% Triton for 45 minutes at room temperature in the dark and rinsed as before. The coverslips were incubated with pan-Cytokeratin antibody (Dako Mouse mAb M0821) (dilution 1:100) in 1X DPBS + 1% BSA + 0.3% Triton for 30 minutes at room temperature and rinsed as before, followed by an incubation with Donkey anti-mouse Alexa Fluor 488 (green) (Molecular Probes A21202) (Dilution 1:600) in 1X DPBS + 1% BSA + 0.3% Triton for 45 minutes at room temperature in the dark. After rinsing as before, the coverslips were incubated with Prolong Gold antifade reagent + DAPI (Molecular Probes P36935) subsequently stored at 4°C in the dark.

2.12. Statistics

Statistics and data visualizations were performed with GraphPad Prism 5 (GraphPad Software Inc., California).

3. Results

This study aimed to establish and characterize in vitro and in vivo models of HGSC for future use in metabolomics experiments. First of all, the carboplatin response of 2 HGSC cell lines was characterized to serve as an in vitro model of platinum resistance. Afterwards, the optimal experimental conditions for a future experiment performed using heavy-isotope labeled nutrients, to track glucose and glutamine fate in both sensitive and resistant cells, were determined. Subsequently, the carboplatin response of 3 PDTX models was characterized and compared to the one observed for the respective original patients. From 1 of these PDTX models, primary PDC cultures were established as a matched in vitro model. The carboplatin response of this in vitro model was also characterized.

3.1. Carboplatin response of 2 HGSC cell lines

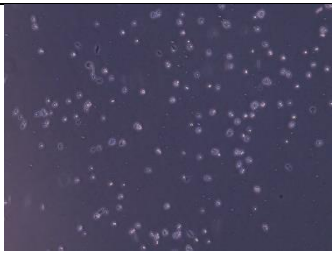

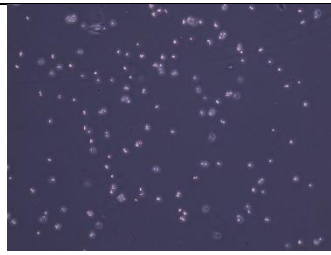
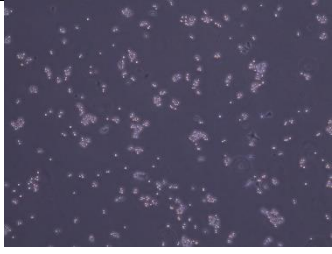



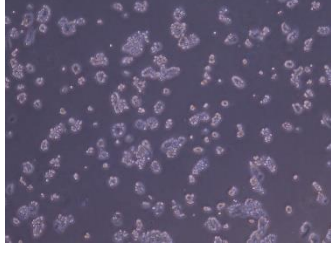
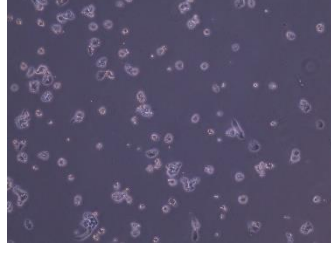
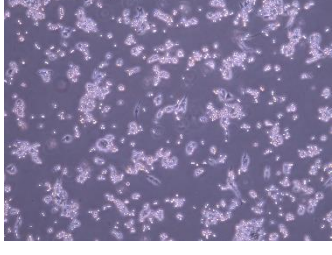

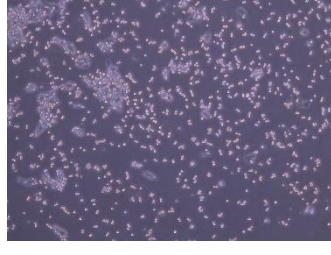
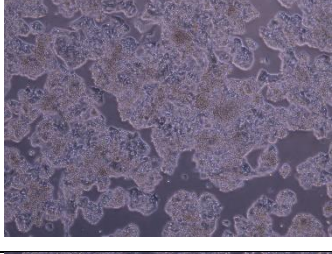
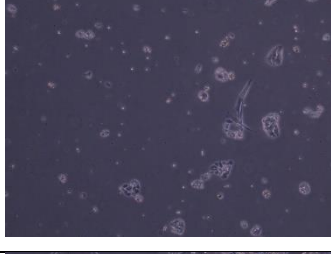
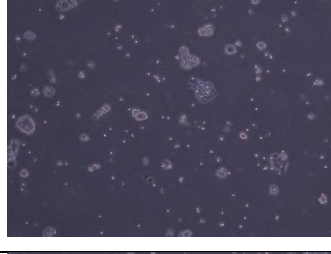
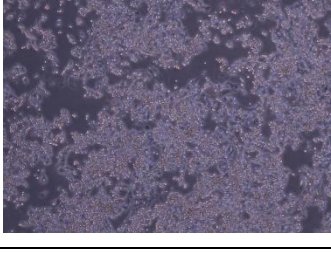

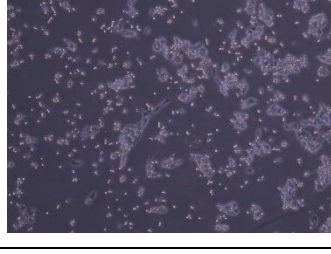
A2780 and A2780 cis are HGSC cell lines, respectively platinum-sensitive and resistant. A2780 is the parental cell line from which A2780 cis was established by chronically exposing the cells to increasing cisplatin concentrations (47).

We plan to use carboplatin instead of cisplatin for the future treatment experiments, both in vitro and in vivo. For this reason, we characterized their response to carboplatin, by assessing the growth rate of both cell lines in the presence of different carboplatin concentration. Subsequently, the concentration of carboplatin needed to inhibit cellular growth by 50% (50% growth inhibitory concentration, GI50) was determined for both cell lines. Finally, the optimal experimental conditions (number of cells seeded and time point of metabolites extraction) were determined.

3.1.1. Dose escalation experiment

To have an idea at which carboplatin concentration A2780 cells growth is inhibited and the one of A2780 cis is not, a dose escalation experiment was performed. The same amount of cells for each cell line was seeded in different wells and subsequently exposed to 0, 0.5, 1, 2, 5 and 10 μM of carboplatin. Pictures were taken daily for 7 days (table 1). At day 4, the growth of A2780 cells appeared to be inhibited both at 5 and 10 μM carboplatin concentration. On the other hand, the A2780 cis cells were able to proliferate at these concentrations. Because 5 μM might be too low to completely inhibit the growth of A2780 cells in a reasonable time for the set up of the metabolomics experiment and 10 μM might be too high, a concentration of 6 μM was selected.

Table 1: Representative pictures of A2780 and A2780 cis cells in control and treatment conditions at selected time points

		0 μ M (control)	5 μ M	10 μ M
Day 0	<u>A2780</u>			
	<u>A2780 cis</u>			
Day 2	<u>A2780</u>			
	<u>A2780 cis</u>			
Day 4	<u>A2780</u>			
	<u>A2780 cis</u>			

3.1.2. Cell growth analysis

Based on the results of the dose escalation experiment, cell growth of A2780 and A2780 cis cell lines was determined in the presence of 6 μ M carboplatin (figure 4). The number of live cells and

percentage of dead cells was assessed daily for 4 days by cell counting and using the trypan blue exclusion assay. The experiment was repeated 3 times.

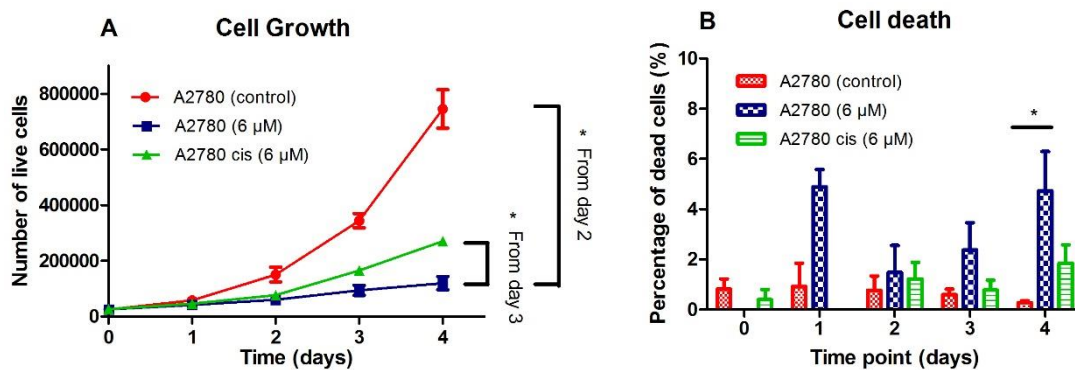


Figure 4: (A) Growth curve for A2780 and A2780 cis cells under carboplatin treatment. Each error bar represents the standard error calculated for 3 independent experiments. (B) Fraction of dead cells for A2780 and A2780 cis in each condition at each time point. Each error bar represents the standard error calculated for 3 independent experiments.

At a concentration of 6 μM of carboplatin, the growth of the sensitive A2780 cell line was inhibited, while A2780 cis cells continued to proliferate. This was also indicated by a difference in the doubling time calculated for the cells under carboplatin treatment (A2780: 46.848 hours, A2780 cis: 28.704 hours). After 4 days of exposure, carboplatin significantly induced cell death in the A2780 cell line ($p = 0.0468$), compared to the untreated condition.

The A2780 cells in control conditions displayed an exponential growth ($R^2 = 0.9656$, exponential curve fit), that was lost when they were treated with 6μM of carboplatin. The A2780 cis cells showed an exponential growth in the presence of 6μM of carboplatin ($R^2 = 0.9735$). From day 2 onwards, there is a significant larger amount of live cells present in the A2780 control condition as compared to the treatment condition ($p = 0.0301$ at day 2. From day 3 onwards, there is a significant difference ($p = 0.0270$ at day 3) between both cell lines treated with carboplatin.

3.1.3. Determination of 50% growth inhibition concentration (GI50)

The 50% growth inhibitory concentration of carboplatin (GI50) was determined for both A2780 and A2780 cis cell lines (figure 5). The cells were exposed to different carboplatin concentrations and growth inhibition was assessed 3 days after exposure by counting the live cells at each concentration. The experiment was repeated 3 times. When cell growth in the absence of carboplatin is taken as 100%, the concentration at which cell growth is reduced to 50% gives the GI50.

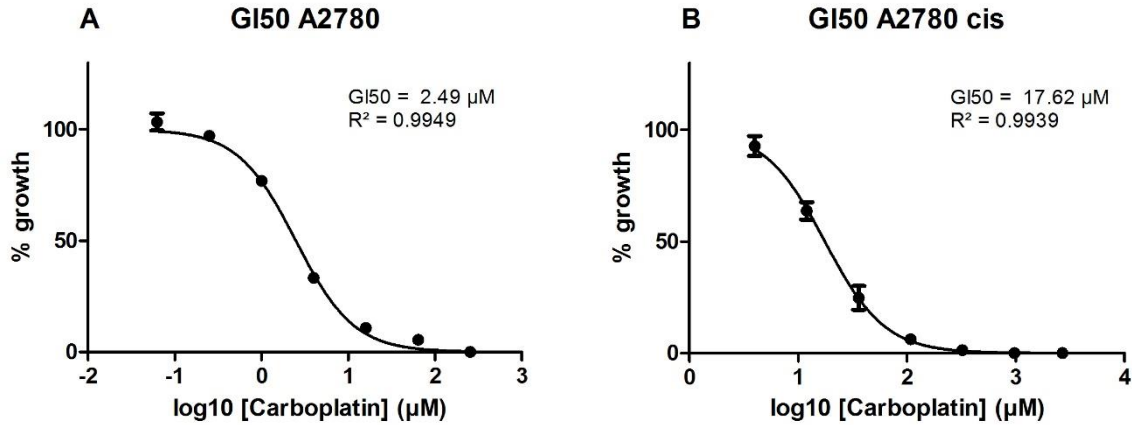


Figure 5: GI50 curve for carboplatin in A2780 (A) and A2780 cis (B) cell lines. Each error bar represents the standard error for 3 independent experiments.

The sensitive A2780 and the resistant A2780 cis cells had a GI50 of 2.49 μM carboplatin (95% CI: 2.263 μM – 2.740 μM) and 17.62 μM carboplatin (95% CI: 16.43 μM – 18.90 μM), respectively. This means that the resistant cell line’s growth is inhibited by 50% at a concentration 7 times higher than the one needed to inhibit the growth of the sensitive cell line.

3.1.4. Cell growth under selected experimental conditions

Metabolites will be extracted from the A2780 and A2780 cis cell lines for further analysis in metabolomics experiments. To determine the optimal time point for metabolites extraction, A2780 and A2780 cis cells’ growth and death were measured under the specific culture conditions that will be used in these future experiments (figure 6). More specifically, on day 2 the corresponding medium on all plates was replaced to mimic addition of medium containing the labeled compounds.

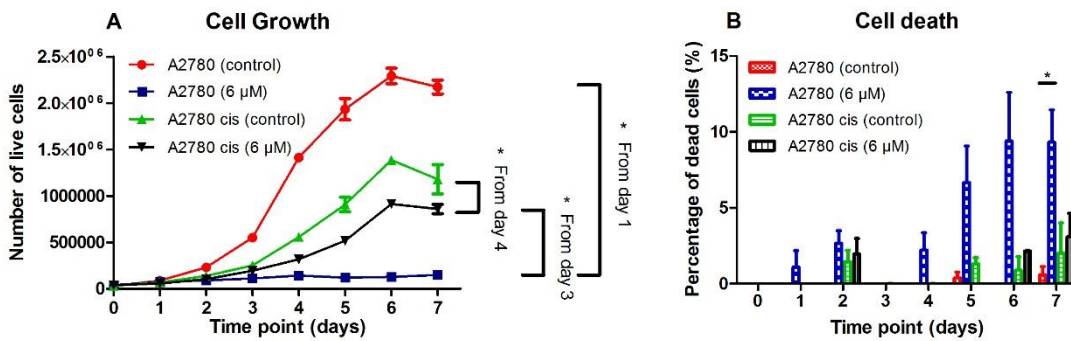


Figure 6: (A) Growth curve for A2780 and A2780 cis cells under carboplatin treatment. Each error bar represents the standard error calculated for 3 independent experiments. (B) Fraction of dead cells for A2780 and A2780 cis in each condition at each time point. Each error bar represents the standard error calculated for 3 independent experiments.

At a concentration of 6 μM of carboplatin, the growth of the sensitive A2780 cell line was inhibited, while the A2780 cis cell line continued to proliferate. In the absence of carboplatin, the sensitive A2780 cell line showed a higher growth rate than the resistant A2780 cis cell line grown without carboplatin, as expected. The absence of dead cells at day 3 was probably caused by the medium change at day 2. At 7 days, the carboplatin caused a significantly higher cell death in the A2780 cell line, compared to its control condition ($p = 0.0166$).

The A2780 cells in the control condition displayed an exponential growth until day 4 ($R^2 = 0.9983$, exponential curve fit). The A2780 cis cells in control and treatment conditions grew exponentially until day 6 ($R^2 = 0.9788$ and 0.9907 respectively). After day 6, all cell lines except A2780 in the treatment condition displayed an absolute decrease in live cell count due to exhaustion of the medium.

From day 1 onwards, there was a significantly larger number of live cells in the A2780 control condition as compared to the treatment condition ($p = 0.0283$ at day 1). From day 4 onwards, there was also a significant difference between the A2780 cis in both conditions ($p = 0.0027$ at day 4). From day 3 onwards, there was a significant difference between both cell lines in treatment conditions ($p = 0.0149$ at day 3).

3.2. Carboplatin response of 3 PDTX models

Three different PDTX models were previously established to serve as an in vivo model of platinum resistance in HGSC. Information about the models and donor patients is shown in table 2.

For the treatment experiments, 25 mice were transplanted for each model. When a tumor reached a volume of 425-450 mm³, the animal was included in the treatment experiment and randomized to receive either carboplatin (50mg/Kg, intraperitoneally injected) or placebo (saline, intraperitoneally injected), once a week for 3 weeks. Tumor's response to carboplatin was monitored by measuring tumor volume changes and it was subsequently compared to the carboplatin response of the original patient tumor. It was also assessed whether a biopsy procedure could be used to collect samples without altering tumor volume changes. This procedure will be useful to collect samples at different time points, in order to be able to study tumors' dynamic adaptation to the treatment(s). Using these samples, metabolic alterations during the treatment can be investigated, without the need to sacrifice animals during treatment. Finally, the structure of each PDTX tumor was compared to that of the original patient tumor using H&E staining.

Table 2: Information about the donor patients

<u>Model name</u>	<u>Tumor type</u>	<u>Treatment history</u>	<u>PFI classification</u>	<u>Localization</u>
OVC005	High-grade serous papillary carcinoma	Complete remission after 6 rounds of Carboplatin/Taxol Platinum-resistant relapse 5 months after last carboplatin treatment	Resistant	Ovary
OVC020	High-grade serous papillary ovarian adenocarcinoma	Complete remission after 6 rounds of Carboplatin/Taxol & 18 months of weekly angiogenesis inhibitor Platinum-sensitive lymph node relapse after 51 weeks	Sensitive	Ovary
OVC034	Lymph node metastasis of high-grade serous papillary ovarian adenocarcinoma		Sensitive	Lymph node

3.2.1. Platinum-resistant model (OVC005)

Of the 25 transplanted mice, 13 mice were included in the non-biopsied cohort and 11 in the biopsied cohort. 1 mouse was not included because it failed to respond to anesthesia during the second biopsy procedure. This made it impossible to include it in the biopsy cohort, since a second biopsy was not performed. Due to the successful first biopsy, it was not possible to include the animal in the control group. The results of the tumor measurements of the non-biopsied and the biopsied cohort are shown in figure 7.

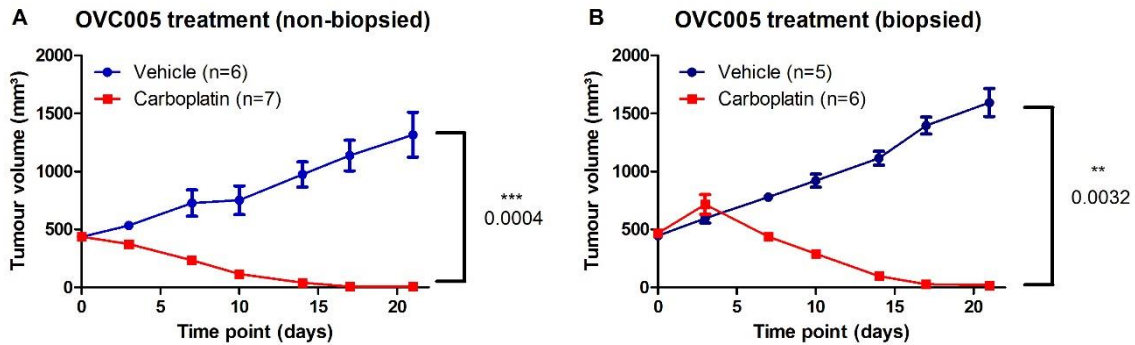


Figure 7: Tumor volume progression during treatment for the mice in the (A) non-biopsied and (B) biopsied cohorts of OVC005. Each error bar represents the standard error for the respective number of data points. Animals were treated at day 0, 7 and 14. Biopsies were performed at day 0 and 10.

In both cohorts, carboplatin treatment caused marked tumor regression. In 11 of the 13 (84.62%) carboplatin-treated mice, there was no palpable tumor mass present after 3 weeks of treatment (minimal residual disease, MRD). This response is comparable to that of the original patient, who had a complete remission after the treatment.

The biopsy procedure did not cause a significant difference between the vehicle and treatment groups in both cohorts ($p = 0.4999$ and 0.3386 respectively).

At the moment this thesis is being presented, in 3 of the mice with MRD there was a tumor relapse. The others are still being monitored. These mice were treated with carboplatin according to the original schedule when the tumor again reached 425 – 450 mm³. The tumor measurements for these 3 mice during the whole experiment are individually shown in figure 8 (time of new treatment start is indicated by arrows).

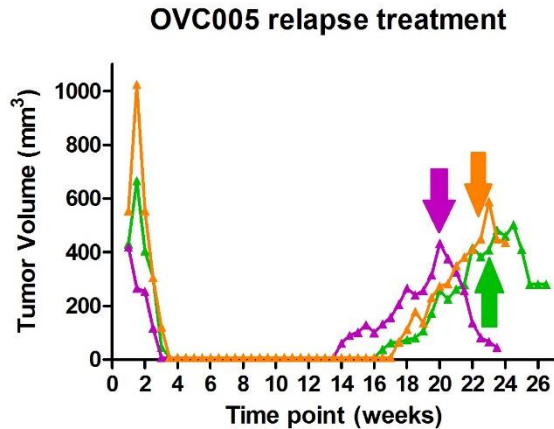


Figure 8: Tumor measurements during the whole experiment for the individual RMD mice in OVC005. Arrows indicate time point of inclusion for the relapsed tumor.

The relapses in the MRD mice occurred between 11 and 14 weeks after the last carboplatin treatment. A similar relapse was seen in the original patient, who relapsed after carboplatin/taxol administration within 5 months from the last treatment. In contrast to the original treatment cohort, the relapsed MRD mice showed different responses to carboplatin. Before the completion of the treatment of one relapsed tumor, the animal had to be sacrificed due to severe weight loss. Dissection did not reveal any macroscopic metastases. This means that it is uncertain whether this animal got sick from the cancer or an alternative cause, like an infection. In 2 cases, the tumor kept growing for 1 week, before it started regressing. In the other case, the tumor responded immediately and regressed. None of the 3 tumors regressed completely before sacrifice 1 week after the last treatment. These different responses probably reflect the heterogeneity of the original tumor.

After sacrifice, tumor sections from placebo-treated mice were stained with hematoxylin & eosin and compared with stained sections from the original patient tumor (figure 9). This way, it was possible to assess whether the PDTX tumor still morphologically resembled the donor tumor.

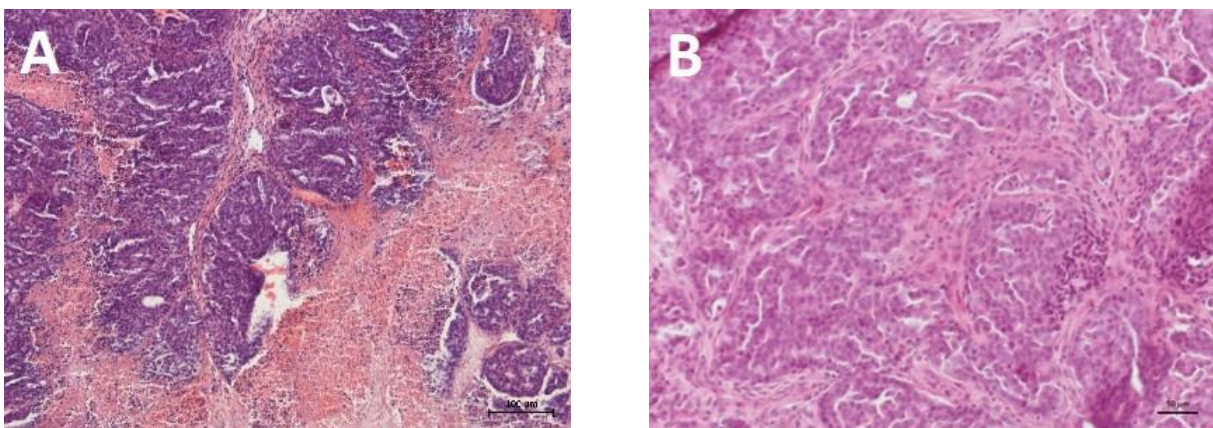


Figure 9: Representative H&E staining of (A) OVC005 tumor and (B) donor patient tumor. Scales show 100 and 50 μm respectively.

Both sections showed a poorly differentiated high-grade serous ovarian carcinoma. In the donor tumor, there were large tumor cells present with nuclei of variable size and papillary structures were identifiable. In the OVC005 tumor, there was less stroma present as compared to the donor tumor,

but papillary structures were also visible. The nuclei were variable in size. The overall architectural morphology of both tumors could be considered comparable.

3.2.2. Platinum-sensitive model (OVC020)

For the OVC020 treatment experiment, the same experimental described for OVC005 was adopted. All 25 transplanted mice were included, 12 in the non-biopsied cohort and 13 in the biopsied cohort. Tumor volume changes for this experiment are shown in figure 10.

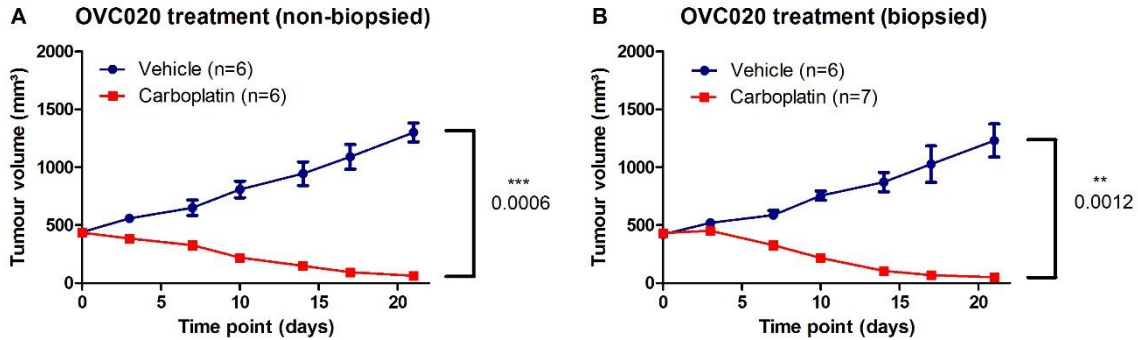


Figure 10: Tumor volume progression during treatment for the mice in (A) non-biopsied and (B) biopsied cohort of OVC020. Each error bar represents the standard error for the respective number of data points. Animals were treated at day 0, 7 and 14. The biopsied cohort was biopsied at day 0 and 10.

In both cohorts, carboplatin treatment caused a decrease of the average tumor volume. The original patient tumor also regressed when treated with carboplatin, with a documented PFI of > 12 months. Of the 13 mice treated with carboplatin, 1 (7.69%) regressed completely to MRD. The biopsy procedure did not lead to a significant difference between placebo and treatments groups in both cohorts ($p = 0.7380$ and 0.9720 respectively).

The MRD mouse relapsed 17.5 weeks after the last carboplatin treatment. This is comparable to the original patient, who also relapsed, leading to metastasis in the lymph nodes. The mouse was re-included when the tumour reached 425 – 450 mm³ and was treated with carboplatin according to the original schedule. The tumor measurements for this individual mouse during the whole experiment are shown in figure 11.

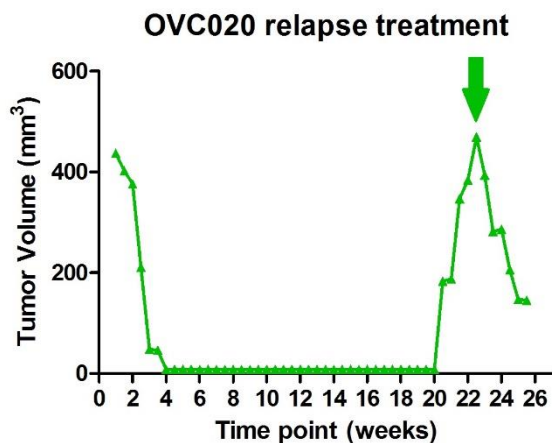


Figure 11: Tumor measurements during the whole experiment for the individual RMD mice in OVC020. Arrow indicates time point

of inclusion of the relapsed tumor.

It is apparent that the tumor volume decreased also during the second round of treatment, which mirrors the carboplatin-sensitivity of the original tumor.

After sacrifice, tumor sections were stained with hematoxylin & eosin and compared with stained slides from the original patient tumor (figure 12).

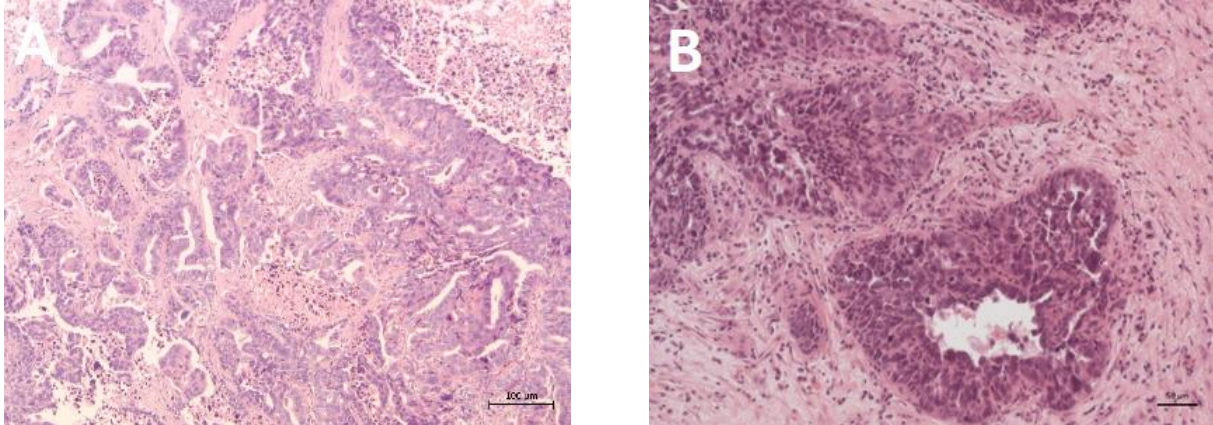


Figure 12: Representative H&E staining of (A) OVC020 tumor and (B) donor patient tumor. Scales show 100 and 50 µM respectively.

Both sections showed a poorly differentiated high-grade serous ovarian carcinoma. In the donor tumor, papillary structures were visible. The cell nuclei were enlarged. In the PDTX tumor, the same papillary structures and large nuclei were visible. The structure of both tumors was considered overall similar.

3.2.3. Relapse model (OVC034)

For the final treatment experiment, OVC034 was used. This model was established using a lymph node relapse tumor from the same patient as OVC020. For this experiment, out of the 25 originally implanted, 10 mice were included in the non-biopsied cohort and 11 in the biopsied cohort. Four animals never developed a tumor. Tumor volume changes for this experiment are shown in figure 13.

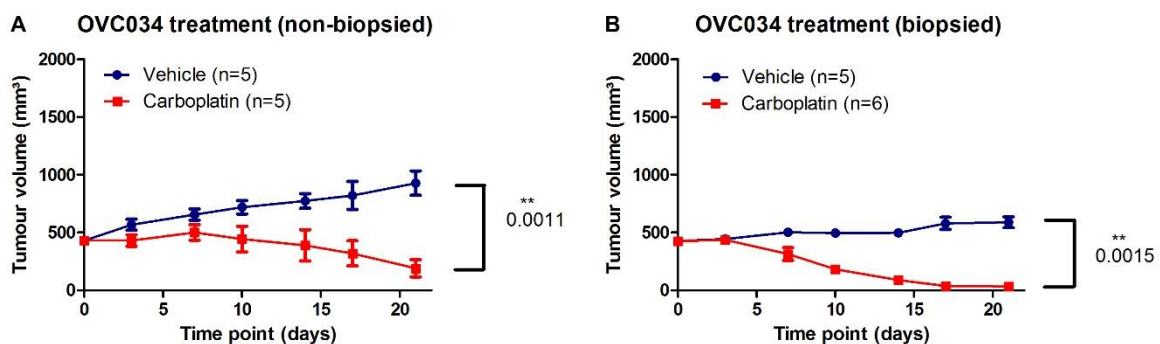


Figure 13: Tumor volume progression during treatment for the mice in (A) non-biopsied and (B) biopsied cohorts of OVC034. Each error bar represents the standard error for the respective number of data points. Animals were treated at day 0, 7 and 14. The biopsied cohort was biopsied at day 0 and 10.

In both the biopsied and non-biopsied cohorts, the average tumor volume of the treatment group decreased over time. Out of the 11 mice treated with carboplatin, 4 (36.37%) had no palpable tumor after treatment. It was not possible to compare the response of the PDTX and patient tumor, since the patient had the lymph node metastasis removed and only after she received the additional platinum treatment.

In contrast to OVC005 and OVC020, there was no strong increase in the average tumor volume in either of the placebo groups, indicating that this specific relapse was a slow-growing tumor. There was a significant difference between placebo and treatment groups in both cohorts.

In this experiment, the biopsy procedure significantly changed the tumor growth in placebo and treatment conditions between both cohorts ($p = 0.0128$ and 0.0473 respectively).

None of the 4 MRD mice relapsed with a visible tumor till the moment this thesis was submitted. However, 1 mouse was sacrificed due to severe weight loss and showed multiple macroscopic metastases along the gastro-intestinal tract.

3.3. Primary PDC culture establishment and carboplatin response

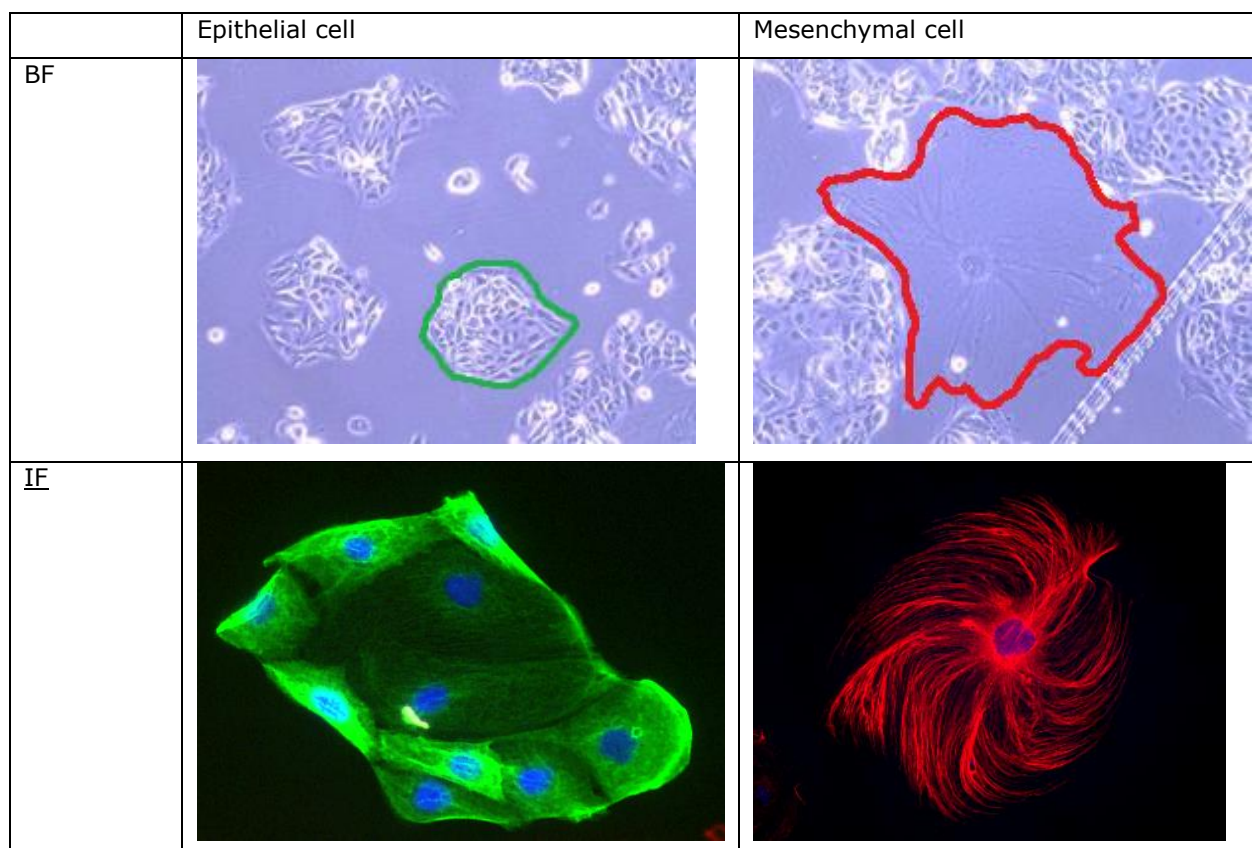
From the resistant PDTX model (OVC005), primary cells were isolated to test their validity as a patient-derived in vitro model. After optimization of the culture protocol, their carboplatin response was characterized using the same procedure adopted for the cell lines' response.

3.3.1. Optimization of culture protocol

To select the optimal culture protocol for the primary OVC005 cells, 2 strategies were evaluated. In strategy 1, cells were first cultivated in non-adherent spheres in serum-free OCMI medium. This medium was optimized from a protocol used in a study by Ince et al. (48), which showed that ovarian cancer cells grow better in OCMI medium than in standard cell culture media. Cells transferred from these conditions to adherent cultures in the presence of serum at 1, 2 and 4 weeks, generally failed to attach and grow. After 6 weeks, it was determined that 75% of cells in the serum-free condition were dead.

In strategy 2, epithelial cells were originally plated in the presence of serum. They attached and started to grow in RPMI + 2% FBS. When the serum concentration was raised to 5% after 2 weeks, epithelial cell growth continued, but regular differential trypsinizations rounds were performed to remove fibroblasts and prevent their overgrowth, since in serum they normally proliferate faster than tumor epithelial cells. After 4 weeks, the serum concentration was raised to 10%. After 3 more weeks of partial trypsinizations, the cell cultures still consisted mostly of 2 cell types (table 3).

Table 3: Representative bright-field (BF) and immunofluorescence (IF) images of different cell types present in the OVC005 culture. For the fluorescent microscopy, cells were stained for DAPI (blue), cytokeratin (green) and vimentin (red).



Strategy 2 resulted in a mixed population mainly consisting of clustered epithelial cells rarely interspersed with large, mononuclear cells with multiple projections. Fluorescent staining confirmed the clustered cells to be epithelial cells because they were cytokeratin-positive. The large cells were deemed to be mesenchymal due to their positivity for vimentin.

3.3.2. Determination of growth rate

Tumor epithelial cells formed the large majority of the cells in OVC005 cell culture. To characterize the response of these cells to carboplatin, a growth curve was established by exposing the cells to 6 μM of carboplatin and following cell growth during a time period of 8 days (figure 14).

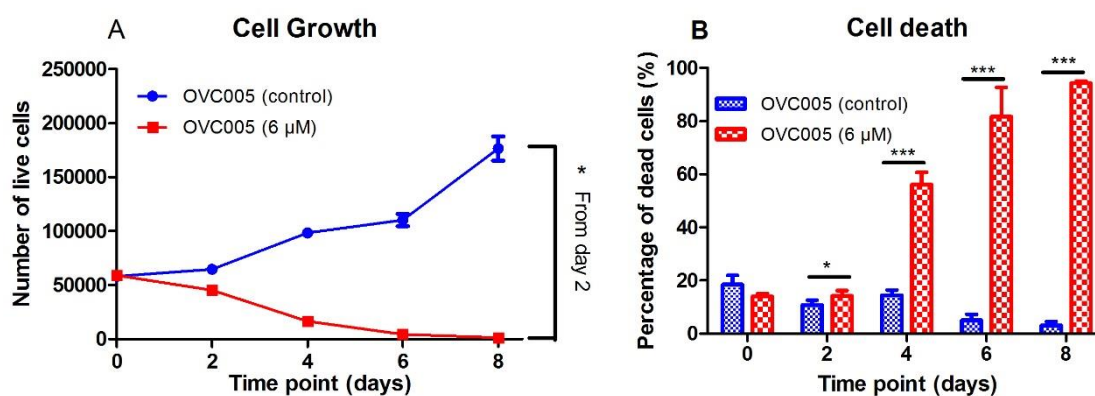


Figure 14: (A) Representative growth curve for OVC005 primary cells in control and carboplatin-exposed conditions. Each error bar represents standard error for 4 replicates within 1 experiment. (B) Fraction of dead cells for OVC005 in each condition at

each time point. Each error bar represents the standard error for 4 replicates.

Carboplatin treatment caused a decrease in the number of live OVC005 cells, over time. This resembled the carboplatin response of the tumor from which the cell culture was derived. From day 2 onwards, carboplatin significantly started to kill the OVC005 cells.

3.3.3. Determination of 50% growth inhibition concentration (GI50)

The 50% growth inhibitory carboplatin concentration (GI50) was determined for the primary OVC005 cells (figure 15). Cells were exposed to different carboplatin concentrations and growth inhibition was assessed 4 days after exposure to carboplatin.

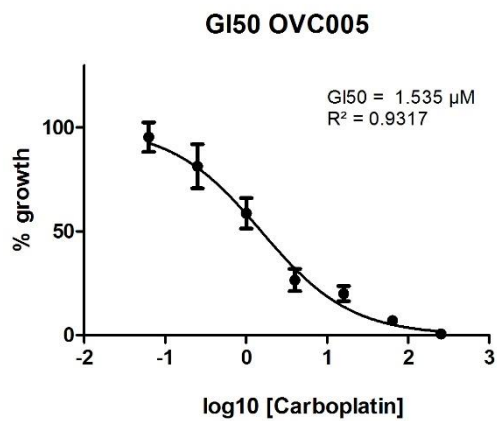


Figure 15: GI50 curve for carboplatin in OVC005 primary cell cultures. Each error bar represents the standard error for 3 data points.

The OVC005 primary cells had a GI50 of 1.535 μM carboplatin (95% CI: 1.045 μM – 2.256 μM).

4. Discussion

Currently, there are no effective treatment for patients with platinum-resistant HGSC. To investigate the impact of metabolic alteration on the resistant phenotype, preclinically-relevant models for platinum resistance in HGSC are needed. For translational research in oncology it is essential to have an easy-to-use in vitro model for initial experiments and patient-derived in vitro and in vivo models to validate the results of these experiments. In this study, the focus was on the establishment and characterization of such models.

4.1. Carboplatin response of HGSC cell lines

The dose escalation experiment showed that, after 4 days, the growth of A2780 cells seemed to be inhibited both at 5 μM and 10 μM carboplatin. At these concentrations, the A2780 cis cells were still able to proliferate. Because of concerns that the A2780 cells would not be completely inhibited at 5 μM and that they would die completely at 10 μM after a longer time period, an in-between concentration of 6 μM carboplatin was selected for future experiments. While this was an arbitrary selection, this concentration fulfilled the main objectives: inhibiting the growth of the sensitive cell line and allowing the resistant cell line to continue proliferating. This will be important for future metabolomics experiments since the platinum concentration should be high enough to activate the resistance mechanism in the resistant cell lines. However, it should not be high enough to kill all the sensitive cells, but it should substantially inhibit their growth, since we are interested in determining the differential route of nutrient utilization in both sensitive and resistant cells, with and without carboplatin administration.

The calculated GI50 for carboplatin was 7 times higher for A2780 cis then for A2780 cells. This higher platinum-resistance of A2780 cis has been seen in previous studies using cisplatin(49, 50). This is expected, since the methods of action of carboplatin and cisplatin are identical (26). This means that cells that are resistant to cisplatin will be probably resistant to carboplatin as well (cross-resistance). However, it is known that a 5 to 10-fold concentration of carboplatin (23, 51) needs to be administered in patients, to have the same effect as cisplatin (52, 53).

The optimal time point for metabolite extraction for labeled tracer experiments was deemed to be between day 4 and day 5, after seeding. At this time point, the A2780 cells are still growing exponentially. According to the results showed, waiting longer would allow these cells to approach the stationary phase, which could have an influence on their metabolism. Between day 4 and 5, the carboplatin was able to inhibit the growth of the sensitive cell line, while the resistant ones still managed to proliferate. We observed a sufficiently large difference between the number of live cells in both cell lines under treatment conditions. Since the A2780 cell line's proliferation was inhibited under carboplatin treatment, a possible concern would be about the detectability of certain metabolites in this condition. This could be solved by seeding more wells of this condition and combining the material of these wells during the experiment.

In the future, these cell lines will be used to perform metabolomics research. In a first phase, the metabolism of labeled glucose and glutamine will be followed in a labeled tracer experiment. Cells will be allowed to metabolize the labeled nutrients for 4 to 5 days. The metabolites will then be then extracted and identified using GC-MS. The metabolite concentrations between both cell lines will be compared to look at significant differences. Metabolites from the TCA cycle and pentose phosphate

pathway are of particular interest. These findings will subsequently have to be validated in an in vivo model.

4.2. Carboplatin response of PDTX models

In all 3 models, carboplatin treatment caused tumor regression while the tumors continued to grow under placebo treatment. In OVC005 and OVC020, this response to carboplatin mirrors that of the respective patients, which also saw regression after the treatment. For OVC034, this cannot be determined since the original lymph node tumor was surgically removed. These results support the pharmacological validity of the models tested. This pharmacological validity is essential since an in vivo model should represent the human response to a drug as closely as possible.

There was a wide variety in the percentage of mice that obtained MRD between the models. This could be the consequence of heterogeneity in the original tumor. A tumor is composed of different cells with a different sensitivity to treatment. When a mouse is transplanted with a piece of tumor that contains a larger subpopulation of resistant cells, it may prove to be more resistant to treatment than a mouse transplanted with a tumor piece with a larger subpopulation of sensitive cells. Additionally, only a relatively small piece of the original patient tumor is transplanted into mice. Finally, there may be a selection for a successful engraftment of more aggressive tumor tissues in some cases.

The MRD OVC005 mice that relapsed showed different responses to carboplatin treatment. This could be caused by the tumor heterogeneity. A tumor that relapsed because of proliferation of a resistant subpopulation will respond differently than one that did so because a small population of sensitive cells survived. The biopsy procedure did not cause changes in the course of tumor growth or regression in 2 of the 3 models (OVC005 and OVC020). This means that in these cases, it can be used as a method to collect tissue samples for future analysis without disturbing the response to carboplatin. In 1 model (OVC034), the biopsy procedure significantly changed the course of tumor volume change. This could be the consequence of the difference in tumor consistencies. While OVC005 and OVC020 were solid tumors, OVC034 regularly showed fluids around the tumor mass. During the biopsy procedure, this fluid leaked, altering the eventual tumor volume.

The structure of the PDTX tumors strongly resembled the one of the original patient tumors. It is known that in PDTX models, after several passages, human stroma is replaced by murine stroma. However, as already shown by others in different tumor types (54), the results of the H&E stainings show that, after several passages, the morphology of the PDTX tumor is still comparable to that of the donor tumor. In addition, KI-67 stainings could determine whether the rate of cell proliferation is comparable between both tumors, while Cleaved caspase-3 is generally used as an apoptotic marker.

In the future, additional OVC PDTX models will be tested in similar treatment experiments. These include models established from patients tumors that are platinum-refractory according to the PFI classification. Additionally, tissue samples and serum collected during the treatment and sacrifice in the current experiments will be analyzed.

4.3. Primary PDC culture establishment and carboplatin response

The established primary OVC005 cell culture consisted of 2 different cell types. Epithelial tumor cells formed the large majority of cells and grew in clones. These epithelial cells were interspersed with large, mesenchymal cells. The stainings that were carried out, do not allow to determine whether these mesenchymal cells were from human or murine origin. To further investigate this, it would be interesting to stain the cells with an antibody specifically targeting human cells. Another option would be to use high-throughput low coverage sequencing to assess what percentage of the cells is of human origin and what percentage is of murine origin.

Because both epithelial and fibroblasts were originally present in the culture at the moment of the isolation procedures, one possibility is that these mesenchymal cells are senescent fibroblasts. It has been previously described that overexpression of vimentin can induce a senescent-like morphology in human fibroblasts (55). Another hypothesis is that these cells are cancer-associated fibroblasts. These cells are present in the tumor microenvironment and play an important role in cancer by promoting processes like tumor growth and metastasis (56). These cells have been implied in the epithelial-mesenchymal transition (57). This hypothesis is supported by the fact that the mesenchymal cells are always surrounded by epithelial cells.

The carboplatin response of the primary cell culture (OVC005) mirrored the one of the corresponding PDX model. Upon carboplatin treatment, the number of live cells decreases significantly due to increases cell death. This supports the validity of this model as a patient-derived in vitro model of carboplatin resistance in HGSC.

In the future, PDCs could be isolated from the additional OVC PDX models present in the lab. Having a collection of different patient-derived in vitro models will provide an important platform for validation of in vivo experimental results. Metabolomics experiments could identify metabolic alterations linked to platinum-resistance by comparing cell cultures of different resistant types. Additionally, these cells could be injected into immune-deficient mice to validate their tumorigenic capabilities.

5. Conclusion

In the present study, we characterized the carboplatin response of 2 HGSC cell lines to enable their use as an easy-to-use in vitro model in future metabolic experiments. Results from these experiments will have to be validated in patient-derived models. To this end we characterized the carboplatin response of 3 PDTX models. We also established a PDC from 1 PDTX model for future use as a patient-derived in vitro model.

In the near future, the HGSC cell lines will be used in a labeled tracer experiment, to determine nutrients fate in carboplatin sensitive and resistant cells. They will be allowed to metabolize labeled glucose and glutamine for 4 to 5 days, after which the metabolites will be extracted. The metabolite concentrations will be analyzed using GC-MS to identify altered metabolites between sensitive and resistant cell lines.

The samples that were collected from the mice during the treatment experiments will also be analyzed for altered metabolites between the different models. Furthermore, additional OVC PDTX models will be established and treated.

Additional PDCs will be established from other OVC PDTX models. Eventually, metabolomics experiments will be performed to identify metabolic alterations between cell cultures with different resistant phenotypes (sensitive, with acquired resistance and refractory). These models also provide a good opportunity to validate in vivo results obtained in a patient-derived in vitro setting.

In conclusion, we successfully characterized the carboplatin response of an in vitro model of HGSC platinum resistance. Additionally, we successfully characterized the carboplatin response of a patient-derived in vitro model and established a patient-derived in vitro model. In the future, these models will be used to study a possible link between metabolic alterations and platinum resistance in HGSC.

References

1. Ferlay J, Shin HR, Bray F, Forman D, Mathers C, Parkin DM. Estimates of worldwide burden of cancer in 2008: GLOBOCAN 2008. *International journal of cancer Journal international du cancer*. 2010;127(12):2893-917.
2. Ferlay J, Steliarova-Foucher E, Lortet-Tieulent J, Rosso S, Coebergh JW, Comber H, et al. Cancer incidence and mortality patterns in Europe: estimates for 40 countries in 2012. *European journal of cancer*. 2013;49(6):1374-403.
3. Kurman RJ, Shih Ie M. The origin and pathogenesis of epithelial ovarian cancer: a proposed unifying theory. *The American journal of surgical pathology*. 2010;34(3):433-43.
4. Jayson GC, Kohn EC, Kitchener HC, Ledermann JA. Ovarian cancer. *Lancet*. 2014;384(9951):1376-88.
5. Berns EM, Bowtell DD. The changing view of high-grade serous ovarian cancer. *Cancer research*. 2012;72(11):2701-4.
6. Ledermann JA, Raja FA, Fotopoulou C, Gonzalez-Martin A, Colombo N, Sessa C, et al. Newly diagnosed and relapsed epithelial ovarian carcinoma: ESMO Clinical Practice Guidelines for diagnosis, treatment and follow-up. *Annals of oncology : official journal of the European Society for Medical Oncology / ESMO*. 2013;24 Suppl 6:vi24-32.
7. Banerjee S, Kaye SB. New strategies in the treatment of ovarian cancer: current clinical perspectives and future potential. *Clinical cancer research : an official journal of the American Association for Cancer Research*. 2013;19(5):961-8.
8. D'Angelo E, Prat J. Classification of ovarian carcinomas based on pathology and molecular genetics. *Clinical & translational oncology : official publication of the Federation of Spanish Oncology Societies and of the National Cancer Institute of Mexico*. 2010;12(12):783-7.
9. Gilks CB, Prat J. Ovarian carcinoma pathology and genetics: recent advances. *Human pathology*. 2009;40(9):1213-23.
10. Davis A, Tinker AV, Friedlander M. "Platinum resistant" ovarian cancer: what is it, who to treat and how to measure benefit? *Gynecologic oncology*. 2014;133(3):624-31.
11. Cooke SL, Brenton JD. Evolution of platinum resistance in high-grade serous ovarian cancer. *The Lancet Oncology*. 2011;12(12):1169-74.
12. Cancer Genome Atlas Research N. Integrated genomic analyses of ovarian carcinoma. *Nature*. 2011;474(7353):609-15.
13. Malpica A, Deavers MT, Lu K, Bodurka DC, Atkinson EN, Gershenson DM, et al. Grading ovarian serous carcinoma using a two-tier system. *The American journal of surgical pathology*. 2004;28(4):496-504.
14. Green DR, Galluzzi L, Kroemer G. Cell biology. Metabolic control of cell death. *Science*. 2014;345(6203):1250256.
15. Vaughan S, Coward JI, Bast RC, Jr., Berchuck A, Berek JS, Brenton JD, et al. Rethinking ovarian cancer: recommendations for improving outcomes. *Nature reviews Cancer*. 2011;11(10):719-25.
16. Bowtell DD, Bohm S, Ahmed AA, Aspuria PJ, Bast RC, Jr., Beral V, et al. Rethinking ovarian cancer II: reducing mortality from high-grade serous ovarian cancer. *Nature reviews Cancer*. 2015;15(11):668-79.
17. Ahmed AA, Etemadmoghadam D, Temple J, Lynch AG, Riad M, Sharma R, et al. Driver mutations in TP53 are ubiquitous in high grade serous carcinoma of the ovary. *The Journal of pathology*. 2010;221(1):49-56.
18. du Bois A, Reuss A, Pujade-Lauraine E, Harter P, Ray-Coquard I, Pfisterer J. Role of surgical outcome as prognostic factor in advanced epithelial ovarian cancer: a combined exploratory analysis of 3 prospectively randomized phase 3 multicenter trials: by the Arbeitsgemeinschaft Gynaekologische Onkologie Studiengruppe Ovarialkarzinom (AGO-OVAR) and the Groupe d'Investigateurs Nationaux Pour les Etudes des Cancers de l'Ovaire (GINECO). *Cancer*. 2009;115(6):1234-44.

19. Miller DS, Blessing JA, Krasner CN, Mannel RS, Hanjani P, Pearl ML, et al. Phase II evaluation of pemetrexed in the treatment of recurrent or persistent platinum-resistant ovarian or primary peritoneal carcinoma: a study of the Gynecologic Oncology Group. *Journal of clinical oncology : official journal of the American Society of Clinical Oncology*. 2009;27(16):2686-91.
20. Lalwani N, Prasad SR, Vikram R, Shanbhogue AK, Huettner PC, Fasih N. Histologic, molecular, and cytogenetic features of ovarian cancers: implications for diagnosis and treatment. *Radiographics : a review publication of the Radiological Society of North America, Inc*. 2011;31(3):625-46.
21. Schorge JO, McCann C, Del Carmen MG. Surgical debulking of ovarian cancer: what difference does it make? *Reviews in obstetrics & gynecology*. 2010;3(3):111-7.
22. ten Bokkel Huinink WW, Dalesio O, Rodenhuis S, Dubbelman R, Hilton A, Franklin H, et al. Replacement of cisplatin with carboplatin in combination chemotherapy against ovarian cancer: long-term treatment results of a study of the Gynaecological Cancer Cooperative Group of the EORTC and experience at The Netherlands Cancer Institute. *Seminars in oncology*. 1992;19(1 Suppl 2):99-101.
23. Lokich J, Anderson N. Carboplatin versus cisplatin in solid tumors: an analysis of the literature. *Annals of oncology : official journal of the European Society for Medical Oncology / ESMO*. 1998;9(1):13-21.
24. Chatelut E. [Pharmacology of platinum compounds: differences between the three molecules and factors of interpatient variability]. *Bulletin du cancer*. 2011;98(11):1253-61.
25. Hoskins PJ, Le N. Identifying patients unlikely to benefit from further chemotherapy: a descriptive study of outcome at each relapse in ovarian cancer. *Gynecologic oncology*. 2005;97(3):862-9.
26. Galluzzi L, Vitale I, Michels J, Brenner C, Szabadkai G, Harel-Bellan A, et al. Systems biology of cisplatin resistance: past, present and future. *Cell death & disease*. 2014;5:e1257.
27. Siddik ZH. Cisplatin: mode of cytotoxic action and molecular basis of resistance. *Oncogene*. 2003;22(47):7265-79.
28. McGuire WP, Hoskins WJ, Brady MF, Kucera PR, Partridge EE, Look KY, et al. Cyclophosphamide and cisplatin compared with paclitaxel and cisplatin in patients with stage III and stage IV ovarian cancer. *The New England journal of medicine*. 1996;334(1):1-6.
29. Horwitz SB. Taxol (paclitaxel): mechanisms of action. *Annals of oncology : official journal of the European Society for Medical Oncology / ESMO*. 1994;5 Suppl 6:S3-6.
30. Safaei R. Role of copper transporters in the uptake and efflux of platinum containing drugs. *Cancer letters*. 2006;234(1):34-9.
31. Liang ZD, Long Y, Tsai WB, Fu S, Kurzrock R, Gagea-Iurascu M, et al. Mechanistic basis for overcoming platinum resistance using copper chelating agents. *Molecular cancer therapeutics*. 2012;11(11):2483-94.
32. Konstantinopoulos PA, Ceccaldi R, Shapiro GI, D'Andrea AD. Homologous Recombination Deficiency: Exploiting the Fundamental Vulnerability of Ovarian Cancer. *Cancer discovery*. 2015;5(11):1137-54.
33. Helleman J, van Staveren IL, Dinjens WN, van Kuijk PF, Ritstier K, Ewing PC, et al. Mismatch repair and treatment resistance in ovarian cancer. *BMC cancer*. 2006;6:201.
34. Bao L, Jaramillo MC, Zhang Z, Zheng Y, Yao M, Zhang DD, et al. Induction of autophagy contributes to cisplatin resistance in human ovarian cancer cells. *Molecular medicine reports*. 2015;11(1):91-8.
35. Cohen M, Dromard M, Petignat P. Heat shock proteins in ovarian cancer: a potential target for therapy. *Gynecologic oncology*. 2010;119(1):164-6.
36. Komurov K, Tseng JT, Muller M, Seviour EG, Moss TJ, Yang L, et al. The glucose-deprivation network counteracts lapatinib-induced toxicity in resistant ErbB2-positive breast cancer cells. *Molecular systems biology*. 2012;8:596.
37. Poisson LM, Munkarah A, Madi H, Datta I, Hensley-Alford S, Tebbe C, et al. A metabolomic approach to identifying platinum resistance in ovarian cancer. *Journal of ovarian research*. 2015;8:13.

38. Sawers L, Ferguson MJ, Ihrig BR, Young HC, Chakravarty P, Wolf CR, et al. Glutathione S-transferase P1 (GSTP1) directly influences platinum drug chemosensitivity in ovarian tumour cell lines. *British journal of cancer*. 2014;111(6):1150-8.
39. Pommier AJ, Farren M, Patel B, Wappett M, Michopoulos F, Smith NR, et al. Leptin, BMI, and a Metabolic Gene Expression Signature Associated with Clinical Outcome to VEGF Inhibition in Colorectal Cancer. *Cell metabolism*. 2016;23(1):77-93.
40. Hidalgo M, Amant F, Biankin AV, Budinska E, Byrne AT, Caldas C, et al. Patient-derived xenograft models: an emerging platform for translational cancer research. *Cancer discovery*. 2014;4(9):998-1013.
41. Xu X, Farach-Carson MC, Jia X. Three-dimensional in vitro tumor models for cancer research and drug evaluation. *Biotechnology advances*. 2014;32(7):1256-68.
42. Gillet JP, Calcagno AM, Varma S, Marino M, Green LJ, Vora MI, et al. Redefining the relevance of established cancer cell lines to the study of mechanisms of clinical anti-cancer drug resistance. *Proceedings of the National Academy of Sciences of the United States of America*. 2011;108(46):18708-13.
43. Fatehullah A, Tan SH, Barker N. Organoids as an in vitro model of human development and disease. *Nature cell biology*. 2016;18(3):246-54.
44. Walrath JC, Hawes JJ, Van Dyke T, Reilly KM. Genetically engineered mouse models in cancer research. *Advances in cancer research*. 2010;106:113-64.
45. Hidalgo M, Bruckheimer E, Rajeshkumar NV, Garrido-Laguna I, De Oliveira E, Rubio-Viqueira B, et al. A pilot clinical study of treatment guided by personalized tumorgrafts in patients with advanced cancer. *Molecular cancer therapeutics*. 2011;10(8):1311-6.
46. Siolas D, Hannon GJ. Patient-derived tumor xenografts: transforming clinical samples into mouse models. *Cancer research*. 2013;73(17):5315-9.
47. Behrens BC, Hamilton TC, Masuda H, Grotzinger KR, Whang-Peng J, Louie KG, et al. Characterization of a cis-diamminedichloroplatinum(II)-resistant human ovarian cancer cell line and its use in evaluation of platinum analogues. *Cancer research*. 1987;47(2):414-8.
48. Ince TA, Sousa AD, Jones MA, Harrell JC, Agoston ES, Krohn M, et al. Characterization of twenty-five ovarian tumour cell lines that phenocopy primary tumours. *Nature communications*. 2015;6:7419.
49. Parker RJ, Eastman A, Bostick-Bruton F, Reed E. Acquired cisplatin resistance in human ovarian cancer cells is associated with enhanced repair of cisplatin-DNA lesions and reduced drug accumulation. *The Journal of clinical investigation*. 1991;87(3):772-7.
50. Godwin AK, Meister A, O'Dwyer PJ, Huang CS, Hamilton TC, Anderson ME. High resistance to cisplatin in human ovarian cancer cell lines is associated with marked increase of glutathione synthesis. *Proceedings of the National Academy of Sciences of the United States of America*. 1992;89(7):3070-4.
51. Lokich J. What is the "best" platinum: cisplatin, carboplatin, or oxaliplatin? *Cancer investigation*. 2001;19(7):756-60.
52. Los G, Verdegaal EM, Mutsaers PH, McVie JG. Penetration of carboplatin and cisplatin into rat peritoneal tumor nodules after intraperitoneal chemotherapy. *Cancer chemotherapy and pharmacology*. 1991;28(3):159-65.
53. Hongo A, Seki S, Akiyama K, Kudo T. A comparison of in vitro platinum-DNA adduct formation between carboplatin and cisplatin. *The International journal of biochemistry*. 1994;26(8):1009-16.
54. Depreeuw J, Hermans E, Schrauwen S, Annibaldi D, Coenegrachts L, Thomas D, et al. Characterization of patient-derived tumor xenograft models of endometrial cancer for preclinical evaluation of targeted therapies. *Gynecologic oncology*. 2015;139(1):118-26.
55. Nishio K, Inoue A, Qiao S, Kondo H, Mimura A. Senescence and cytoskeleton: overproduction of vimentin induces senescent-like morphology in human fibroblasts. *Histochemistry and cell biology*. 2001;116(4):321-7.
56. Madar S, Goldstein I, Rotter V. 'Cancer associated fibroblasts'--more than meets the eye. *Trends in molecular medicine*. 2013;19(8):447-53.

57. Yu Y, Xiao CH, Tan LD, Wang QS, Li XQ, Feng YM. Cancer-associated fibroblasts induce epithelial-mesenchymal transition of breast cancer cells through paracrine TGF-beta signalling. *British journal of cancer*. 2014;110(3):724-32.

Auteursrechtelijke overeenkomst

Ik/wij verlenen het wereldwijde auteursrecht voor de ingediende eindverhandeling:

Establishment and characterization of high-grade serous ovarian cancer models to study the role of metabolic adaptations in platinum resistance

Richting: **master in de biomedische wetenschappen-klinische moleculaire wetenschappen**

Jaar: **2016**

in alle mogelijke mediaformaten, - bestaande en in de toekomst te ontwikkelen - , aan de Universiteit Hasselt.

Niet tegenstaand deze toekenning van het auteursrecht aan de Universiteit Hasselt behoud ik als auteur het recht om de eindverhandeling, - in zijn geheel of gedeeltelijk -, vrij te reproduceren, (her)publiceren of distribueren zonder de toelating te moeten verkrijgen van de Universiteit Hasselt.

Ik bevestig dat de eindverhandeling mijn origineel werk is, en dat ik het recht heb om de rechten te verlenen die in deze overeenkomst worden beschreven. Ik verklaar tevens dat de eindverhandeling, naar mijn weten, het auteursrecht van anderen niet overtreedt.

Ik verklaar tevens dat ik voor het materiaal in de eindverhandeling dat beschermd wordt door het auteursrecht, de nodige toelatingen heb verkregen zodat ik deze ook aan de Universiteit Hasselt kan overdragen en dat dit duidelijk in de tekst en inhoud van de eindverhandeling werd genotificeerd.

Universiteit Hasselt zal mij als auteur(s) van de eindverhandeling identificeren en zal geen wijzigingen aanbrengen aan de eindverhandeling, uitgezonderd deze toegelaten door deze overeenkomst.

Voor akkoord,

Stans, Jelle

Datum: **8/06/2016**